Lawrence Berkeley Laboratory
UNIVERSITY OF CALIFORNIA

Materials & Molecular Research Division

Submitted to Applied Optics

NEAR-MILLIMETER WAVE BAND-PASS FILTERS

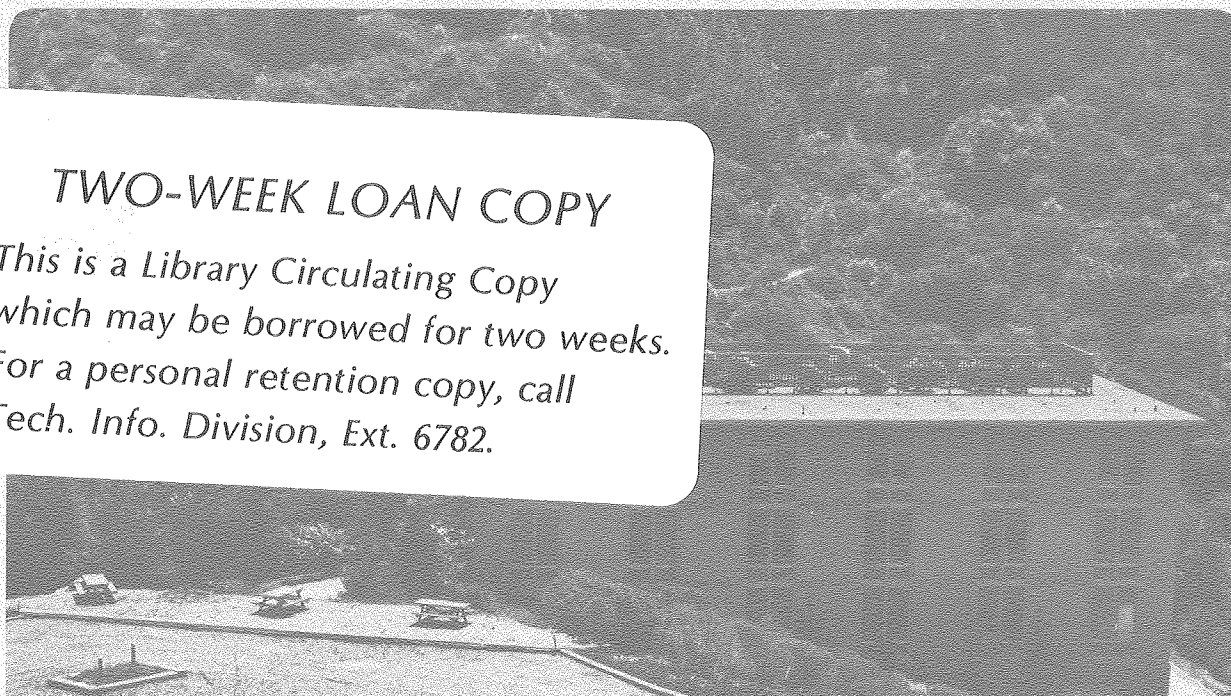T. Timusk and P.L. Richards

November 1980

DISCLAIMER

NEAR-MILLIMETER WAVE BAND-PASS FILTERS

T. Timusk* and P. L. Richards

Department of Physics, University of California
Berkeley, California 94720.

ABSTRACT

We report on the properties of band-pass filters for broad band photometry in the frequency range from 3 to $12cm^{-1}$. The filters are based on a combination of capacitive grids deposited on thick Mylar substrates and are designed to have very high out-of-band rejection. Low frequencies are blocked by a "thick grill" that consists of hexagonal grid of circular holes in a thick metal plate.

I. Introduction

A filter used for band photometry in the millimeter wave region often needs a broad pass-band to collect a useful amount of energy. At the same time it should have very low leakage at high frequencies to block radiation from hot sources, especially if the photometer is to be calibrated with a warm black body. In this paper we report on a band-pass filter design that meets these requirements, a design based on capacitive grids deposited on opposite sides of a dielectric substrate. To provide low frequency blocking for the filter we also describe a new inductive element, the thick grill.

*Present address of T. Timusk is McMaster University, Department of Physics, Hamilton, Ontario, Canada L8S 4M1.

The capacitive grid is a periodic pattern of metal squares evaporated on the surface of a dielectric substrate. It has been widely used in low-pass filters for submillimeter wave spectroscopy[1-6]. The usual low-pass filter consists of several grids separated either by air or by the dielectric substrates. It has excellent low frequency transmittance and high frequency blocking. With four equally spaced grids the filter has considerable ripple in the pass-band which can be suppressed by a suitable choice of filter elements[3]. On the other hand, the ripple can be accentuated by a careful choice of element spacings. In this way a band-pass filter can be developed. We find that by placing pairs of grids close together, for example on the opposite sides of a dielectric substrate, and separating the substrates by one quarter of the center wavelength of the desired pass-band, the highest frequency maximum in the pass-band is enhanced at the expense of other maxima.

The resulting filter resembles two Fabry-perot interferometers in series, each used in first order. The orders are not equally spaced in frequency and the optical thickness of the substrate is significantly less than a half wavelength, because of the large frequency-dependent phase shift on reflection from a capacitive grid. The large zero order and small second order response of this structure are blocked with additional high- and low-pass filters and a proper choice of the period of the capacitive mesh.

The dielectric substrate we use to separate the closely spaced elements has important effects on the properties of the filter. The dielectric lowers the grid impedance[7] since it increases the capacitance between the individual square elements of the grid. This leads to increased reflectance and decreased transmittance. As a result, the band-pass region becomes narrower. The transmission is reduced, but more strongly

in the stop-band than in the pass-band. Since the separation between the closely spaced elements is fixed by the thickness of the dielectric, the resulting structure is very robust. The shape and transmission of the pass band is relatively insensitive to the distance between the dielectric elements, provided this separation is the order of $\lambda/4$.

The thick grill inductive filter was developed to block the region of low frequencies where the capacitive grid is transparent. It consists of a thick metal plate with a hexagonal close-packed array of circular holes. A thin inductive mesh would serve the same purpose, but it does not have as sharp a cutoff. The thick grill used here does not transmit frequencies below the lowest frequency propagating circular waveguide modes in the holes. There is a transmittance maximum at $\nu \sim 1/g$, where g is the repetition period of the holes. If this maximum is matched to the maximum of the capacitive grid filter, excellent attenuation of frequencies below the pass-band can be obtained with little sacrifice of the in-band transmittance.

We will summarize the elements of transmission line formalism that apply to multielement filters in the next section. In section III we present some results of calculations and measurements of capacitive band-pass filters and in section IV the measured transmittance of the thick grill filter is presented.

II. Transmittance of a Multigrid Filter

A grid filter can be represented by a combination of equivalent circuit elements with shunt admittances Y, joined by sections of transmission line of length d that represent the dielectric. The transmission lines have a characteristic admittance $Y_d = n_d$, where n_d is the index of refraction. We take all admittances to be relative to the admittance of vacuum, $Y_o = 1$.

Since the capacitive grids are evaporated on the surface of a dielectric, their admittances will depend on the dielectric constant of the substrate, $\varepsilon_d = n_d^2$. The admittance of a capacitive grid deposited on the surface between a medium with index of refraction n_1 and a medium with index of refraction n_2 is increased by the factor $(n_1^2 + n_2^2)/2$. This follows from the elementary argument that leads to the capacitance of a parallel combination of two capacitors with different dielectrics. In contrast, as Ulrich et al.[8] pointed out, the admittance of an inductive grid on the face of a dielectric is independent of the dielectric constant.

A single capacitive grid between two dielectrics can be represented by the equivalent circuit shown in Fig. 1. It was found by Ulrich[1] that this circuit accurately reproduces the frequency-dependent reflectivity of a grid deposited on a very thin substrate over a wide range of frequencies. The parameters and definitions of Fig. 1 generally follow Ulrich, but have been modified to include the factor $(n_1^2 + n_2^2)/2$ which allows for the dielectric, to change the definition of Y to be consistent with usage in transmission line theory[9,10], and to correct a numerical error in the argument of the cosecant function for Y_o[11].

The transmittance of a filter that consists of multiple grids of the type shown in Fig. 1 can be calculated very conveniently by using matrix methods. Figure 2 shows the circuit element represented as a two-port device. The incident wave amplitudes from the left and the right are a_1 and a_2 respectively. The reflected wave amplitudes are b_1 and b_2. The following linear relationships apply

$$b_1 = r_{11}a_2 + r_{12}b_2,$$
$$a_1 = r_{21}a_2 + r_{22}b_2.$$

(1)

The coefficients r_{ij} define the cascading matrix $\tilde{r}$. The reflectivity for a wave coming from the left is $b_1/a_1 = r_{12}/r_{22}$ and the amplitude transmittance is $1/r_{22}$. The cascading matrix is particularly useful in multielement structures since it gives the variables at port 1 in terms of those at port 2, and because the cascading matrix of two transmission line elements that follow one another is simply the product of the individual cascading matrices[10]. To calculate the overall transmittance of a long sequence of circuit elements one simply evaluates the cascading matrix of each element and multiplies the matrices to get an overall cascading matrix. The transmittance and reflection of the overall-circuit can then be evaluated from the elements of this overall matrix.

The cascading matrix for a shunt admittance Y at the junction of two transmission lines of characteristic admittances $Y_1 = n_1$ and $Y_2 = n_2$ is

$$\tilde{r}(Y) = \frac{1}{2n_1} \begin{vmatrix} -Y + (n_1+n_2) & -Y + (n_1-n_2) \\ Y + (n_1-n_2) & Y + (n_1+n_2) \end{vmatrix} . \tag{2}$$

A section of lossless transmission line of length d with the characteristic admittance Y=n is represented by

$$\tilde{r}(d) = \begin{vmatrix} e^{-j\gamma} & 0 \\ 0 & e^{+j\gamma} \end{vmatrix} , \tag{3}$$

where $\gamma = 2\pi n d/\lambda$ and λ is the vacuum wavelength of the wave. If the medium is absorbing, a negative imaginary part must be added to γ.

We have written a simple computer program that uses complex arithmetic to multiply a number of complex 2x2 matrices to represent the filter elements and the spaces. A dielectric surface that has no grid is represented by a cascading matrix with Y=0.

III. Near-Millimeter Wave Band-Pass Filters

There are several possible choices for the dielectric substrate
material. We have built filters on substrates of silicon, glass and Mylar[12].
While silicon and glass have excellent mechanical properties and can be
polished with accurate plane parallel faces, their high indices of refraction
shown in Table I cause difficulties. First, the required thickness of the
filter element is very small. For example, a typical 200μm thick silicon
element has a transmittance peak at 2.7cm^{-1} and a 200μm thick glass filter
at 3.3cm^{-1}. To work at higher frequencies the elements must be made thinner,
a difficult task if the lateral dimension is required to be large. In addition,
a high index of refraction leads to grids with high reflectance and thus
narrow pass-bands.

Mylar proved to be an excellent substrate material for the band-pass
filters in the 5-15cm^{-1} range. It is commercially available in sheet form
in a variety of thicknesses up to 350μm. Small areas can be found by
selection that are plane parallel to one fringe of visible light. We
used 15mm diameter Mylar sheets with thicknesses from 50μm to 350μm as substrates
for the grids. The grids were formed by the vacuum evaporation of aluminum
to a layer thickness of 0.1μm using a commercial inductive grid as a mask.
The substrates were turned over and a second grid evaporated on the opposite
side. No special precautions were taken to align the grids on the opposite
faces other than the rejection of filters with a very large scale Moiré
pattern, a sign of near-alignment of the two elements. The Mylar elements
were spaced by brass rings and the whole assembly mounted under spring com-
pression in a brass holder.

Figure 3 shows the measured transmission at $1.2^{\circ}K$ of several band-pass filters designed to cover the millimeter wave region from $3cm^{-1}$ to $10cm^{-1}$. Table 2 summarizes the properties of the filters used. The choice of peak wavelengths is restricted somewhat by the availability of substrates and inductive mesh evaporation masks. The only continuously adjustable parameter is the thickness of the spacer. The frequency of the peak trans-mittance can be shifted by 5 to 10% by the choice of different spacers; a thinner spacer shifts the peak transmittance to higher frequencies. A thinner substrate also shifts the resonance peak to a higher frequency. The grid has an influence on the position of the resonance as well. In general a high grid admittance (high dielectric constant, narrow gaps between the squares) leads to a lower frequency of resonance and a lower overall transmittance. Similarly, if the grid constant is increased, the transmittance is lowered and the resonance frequency is reduced.

The theory outlined in section II can be used as a guide to the selection of filter parameters. The equivalent circuit used does give a qualitative representation of the filters, but there is a tendency for the peak frequencies of the actual filters to be slightly lower than predicted by the theory. This effect can be described by allowing the normalized frequency ω_0 to deviate from $2\pi/g$. The best fit to the data was obtained by setting $\omega_0 = 0.83 \times 2\pi/g$. The dashed curves of Fig. 3 are the results of calculations with the equivalent circuit of Fig. 1 with the value of ω_0 adjusted this way.

The transmittance of the filters is reduced to some extent by the high absorption of Mylar at near-millimeter wavelengths. Figure 4 shows the room temperature absorption coefficient of a typical sample of sheet Mylar. The calculated curves in Fig. 3 include this absorption. It has

the effect of reducing the peak transmittance of the filters by 30%, in good agreement with the measurements, particularly for the 9.0 and 10.2cm^{-1} filters. The peak transmittance of the lower frequency filters is not predicted so well by the theory, partly due to reduced accuracy of the measurements at low frequencies, but possibly also due to structure in the absorption coefficient of Mylar. We have not explored the frequency dependence of the Mylar absorption at low temperatures. Polyethylene and Teflon have substantially lower absorption coefficients at near-millimeter wavelengths and may be more suitable for applications where high transmittance is a requirement.

Theory also predicts that the overall transmittance of the filters decreases to a minimum that occurs at $\nu=1/g$. The filters are predicted to become transparent again at higher frequencies. The simple equivalent circuit is not valid for $\nu>1/g$ and we did not compute the high frequency region. A six element filter with random angular orientation of the elements is very opaque to visible light. To provide further infrared blocking we add a 3mm thick layer of soda-lime glass and several layers of black polyethylene to the filter. The absorption coefficient of soda-lime glass is shown in Fig. 5.

IV. Thick Grill Filter

The thick grill filter consists of a hexagonal close-packed array of holes drilled in a brass plate whose thickness was two hole diameters. We observed little difference in the transmission curves for a thinner (1.5 hole diameter) plate. Figure 6 shows the transmittance curve for typical thick grill filter with a 1.4mm diameter holes on a 1.6mm spacing. The curve shown was measured at room temperature, but the filter transmission did not change on cooling to 1.2K.

Below the cutoff frequency ν_c = 0.586/d for the lowest propagating mode in a circular waveguide with diameter d, the filter has a very low transmittance. An approximate formula is given by Marcuvitz [9], which is valid for $\nu \ll \nu_c$. The power transmission coefficient of a hole in a thick plate is equal to that of a hole in a thin plate plus a thickness correction of -32.0 db per diameter of the hole. For the filter in Fig. 6, the formula gives a transmittance of 10^{-7} for frequencies well below the cutoff. The transmittance rises rapidly as the cutoff frequency is approached and has a well defined peak. The frequency of the primary peak is directly related to the diameter of the holes and occurs at approximately $\nu = 1.2\nu_c$. The value of the transmittance at the peak, which is 0.84 for the filter in Fig. 6, depends on the ratio of d/g. It exceeds the ratio of hole area to filter area of 0.72. There is obviously a resonance at $\nu \sim 1/g$ that contributes to the high transmittance of this filter.

The decreasing transmittance at higher frequencies is probably related to diffraction of radiation from the regular grid pattern. For $\nu \sim 1/g$ there are no diffracted sidewaves. The beam is all directed in the forward direction and reaches the detector. At higher frequencies $\nu > 1/g$ the first order grating diffraction maxima appear at large angles which do not reach the detector and subtract energy from the zero order beam, so the filter transmission drops. In general we find a small secondary bump just above $\nu = 1/g$ in the transmittance of all of the filters which may be associated with the appearance of the n=1 sidewave. For $\nu \gtrsim 3/g$ the angle of the first order maxima is sufficiently small to reach the detector.

We have made several filters with peak transmission frequencies up to $18cm^{-1}$ and have found that the curve of Fig. 6 is followed rather closely for filters with the same d/g ratio. The frequency scale is then inversely proportional to d, the size of the holes.

The thick grill should find applications other than as a component of our band-pass filters. It can be combined with any low pass filter, such as a Yoshinaga[6] filter, or a capacitive grid low pass filter, to form a very broadband filter. It can also be used as a dichroic reflector to extract the long wavelength portion of a beam. Since the filter is an artificial dielectric medium it can be given focussing properties by curving the surface. If micron size holes can be made in thin aluminum the thick grill will form an excellent hot mirror for a solar collector since it will reflect infrared completely and still have reasonable visible transmission with a very sharp change-over region.

V. Combined Capacitive Grid and Thick Grill Filters

The two filters together form an ideal combination for a band-pass filter. The capacitive grid has a well defined peak and excellent high frequency rejection. The thick grill also has a peak with nearly perfect low frequency rejection. The combined filter has a transmission of approximately 0.5 at the peak frequency, a fractional band width $\Delta v/v$ between 0.2 and 0.4 and steep fall-off of transmission on each side of the pass-band. The actual transmission in the stop-bands is difficult to measure accurately. We expect the transmission of the filters at frequencies above $12cm^{-1}$ to be less than 0.1%. The low frequency stop band should have an even lower transmission.

Figure 7 shows the response of a set of combined filters designed for a balloon-borne measurement of the cosmic microwave background radiation. A set of discrete bands have been chosen to span the frequency range from $3cm^{-1}$ to $10cm^{-1}$ and avoid the atmospheric oxygen features at $2cm^{-1}$ and $4cm^{-1}$. The curves give the overall response of the system consisting of the antenna, a Winston concentrator, the filters, and a ^{3}He temperature composite bolometer. The filters used are the capacitive grids of table 2 labelled 2.8, 5.0, 6.7, 9.0 and 10.2 with matching thick grill filters. Black polyethylene and a 3mm thick soda lime glass are included in the beam path. The filter system also incorporates additional layers of Mylar for anti-reflection coating of the 3mm glass filter, black polyethylene and a Mylar chopper blade with alternately aluminized sectors. The effects of all these elements have been included in the response curves of Fig. 7.

References

1. R. Ulrich, Infrared Phys. $\underline{7}$, 37 (1967).

2. R. Ulrich, Infrared Phys. $\underline{7}$, 65 (1967).

3. R. Ulrich, Applied Optics $\underline{7}$, 1987 (1968).

4. D. Muehlner and R. Weiss, Phys. Rev. D $\underline{7}$, 326 (1973).

5. S. E. Whitcomb and J. Keene, App. Optics $\underline{19}$, (1980).

6. K. D. Möller and W. G. Rothschild, Far Infrared Spectroscopy, (Wiley, New York, 1971), p. 106.

7. V. Y. Balakhanov, Sov. Phys. Doklady $\underline{10}$, 788 (1966).

8. R. Ulrich, K. F. Renk, and L. Genzel, IEEE Trans. MTT-11, 363 (1963).

9. N. Marcuvitz, Waveguide Handbook, MIT Radiation Laboratory Series 10, (McGraw-Hill, New York, 1951).

10. D. M. Kearns and R. W. Beatty, Basic Theory of Waveguide functions and Introductory Microwave Network Analysis, (Pergamon Press, Oxford, 1967).

11. This function is given incorrectly in Ref. 1, 2 and 6. The expressions in Ref. 7 and 9 are correct.

12. Mylar is a trade name for polyethylene terephthalate.

Table I. Millimeter wave indices of refraction of some common dielectrics.

Material	n	Reference
Germanium	4.00	a
Silicon	3.42	a
Glass	2.30	b
Mylar	1.73	d
Polyethylene	1.52	e
Teflon	1.38	f

a) C. M. Randall and R. D. Rawcliffe, Appl. Opt. 6, 1889 (1967).

b) Typical of soda lime glasses, this work.

d) E. V. Loewenstein and D. R. Smith, Appl. Opt. 10, 577 (1971).

e) D. R. Smith and E. V. Loewenstein, Appl. Opt. 14, 1335 (1975).

f) J. E. Chamberlain and H. A. Gebbie, Appl. Opt. 5, 393 (1966).

Table II.   Properties of filters with Mylar substrate shown in Fig. 3.

Pass Band cm^{-1}	Number of Grids	g mm	z_0	substrate mm	spacer mm
2.8	6	0.508	0.281	0.356	1.000
3.8	6	0.508	0.281	0.254	0.500
5.0	6	0.508	0.281	0.127	0.495
6.7	4	0.282	0.294	0.127	0.250
9.0	6	0.282	0.294	0.076	0.178
10.2	6	0.254	0.336	0.076	0.236

Figure Captions

Fig. 1. The equivalent circuit of a thin capacitive grid on the surface separating two dielectrics with admittances $Y_1 = n_1$ and $Y_2 = n_2$.

Resonant frequency	$\omega_0 = 2\pi/g$
Normalized impedance of L and C at resonance	$Z_0 = \omega_0 L = 1/\omega_0 C$
Generalized frequency	$\Omega = \omega/\omega_0 - \omega_0/\omega$
Normalized Admittance	$Y = 1/(R + jZ_0\Omega)$
Grid Admittance	$Y_0 = 1/Z_0 = 2(n_1^2 + n_1^2)\ln\csc(\frac{\pi a}{g})$

Fig. 2. Transmission line shunted by an equivalent admittance Y. The incident wave amplitudes are a_1 and a_2, and the reflected wave amplitudes b_1 and b_2.

Fig. 3. Transmission of a series of Mylar band-pass filters at 1.2K. Each curve is labeled by the center frequency of the pass-band. All measurements were done using a polarizing interferometer at a nominal resolution of 0.4cm^{-1}. The solid curves are the measured filters, while the dashed lines result from a calculation using the equivalent circuit of Fig. 1 with an effective resonant frequency $\omega_0 = 0.83 \times 2\pi/g$. The parameters of the various filters are given in Table II.

Fig. 4. Near-millimeter absorption coefficient of Mylar. The measurement was made on a compressed stack of 20 sheets of 0.25mm thick Mylar. Calculations show that these data are not sensitive to gaps between the sheets as large as 1μm.

Fig. 5. Near-millimeter absorption coefficient of soda-lime glass. The absorption coefficient is less than $1.0cm^{-1}$ between 3 and $8cm^{-1}$.

Fig. 6. Transmission of a thick grill filter. This high pass filter consists of a pattern of 1.4mm diameter holes on a 1.6mm spacing. The thickness is 3mm. The filters act as a series of circular waveguides beyond cutoff. The filter has a well defined peak with a transmission of 0.84 at $\nu \sim 1/g$.

Fig. 7. Overall responsivity of a system designed to measure the cosmic microwave background from a balloon. Five Mylar grid filters are used in combination with matched thick grill filters to produce the pass bands shown. The system includes soda-lime glass and black polyethylene for high frequency blocking. A ^{3}He temperature composite bolometer is used as detector. The data were measured with a nominal resolution of $0.4cm^{-1}$. The spectral output of our polarizing interferometer was assumed to be $\propto \nu^{2}$ and the constant of proportionality was evaluated by measuring the signal from a laboratory black body.
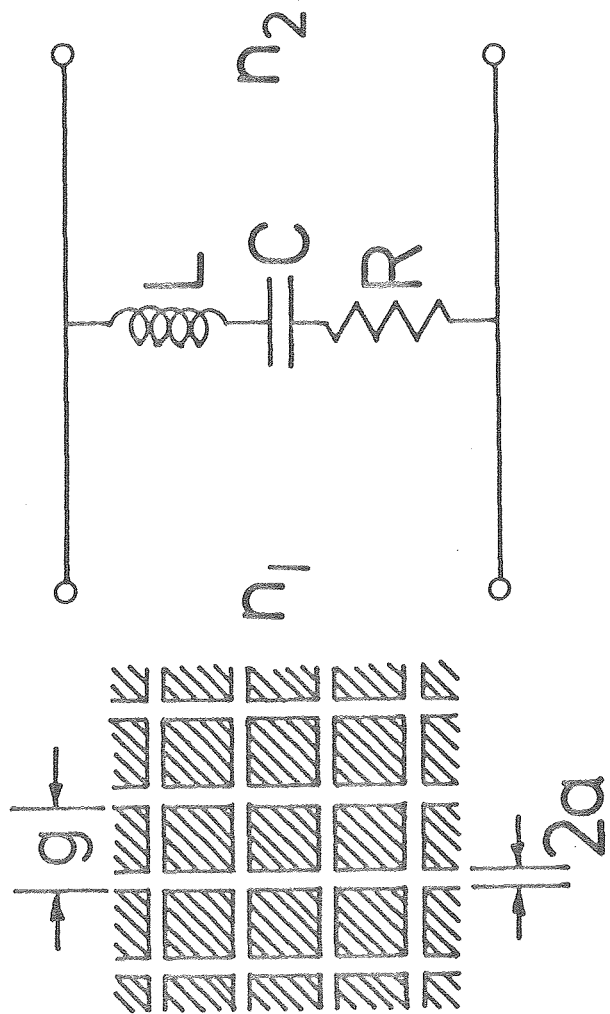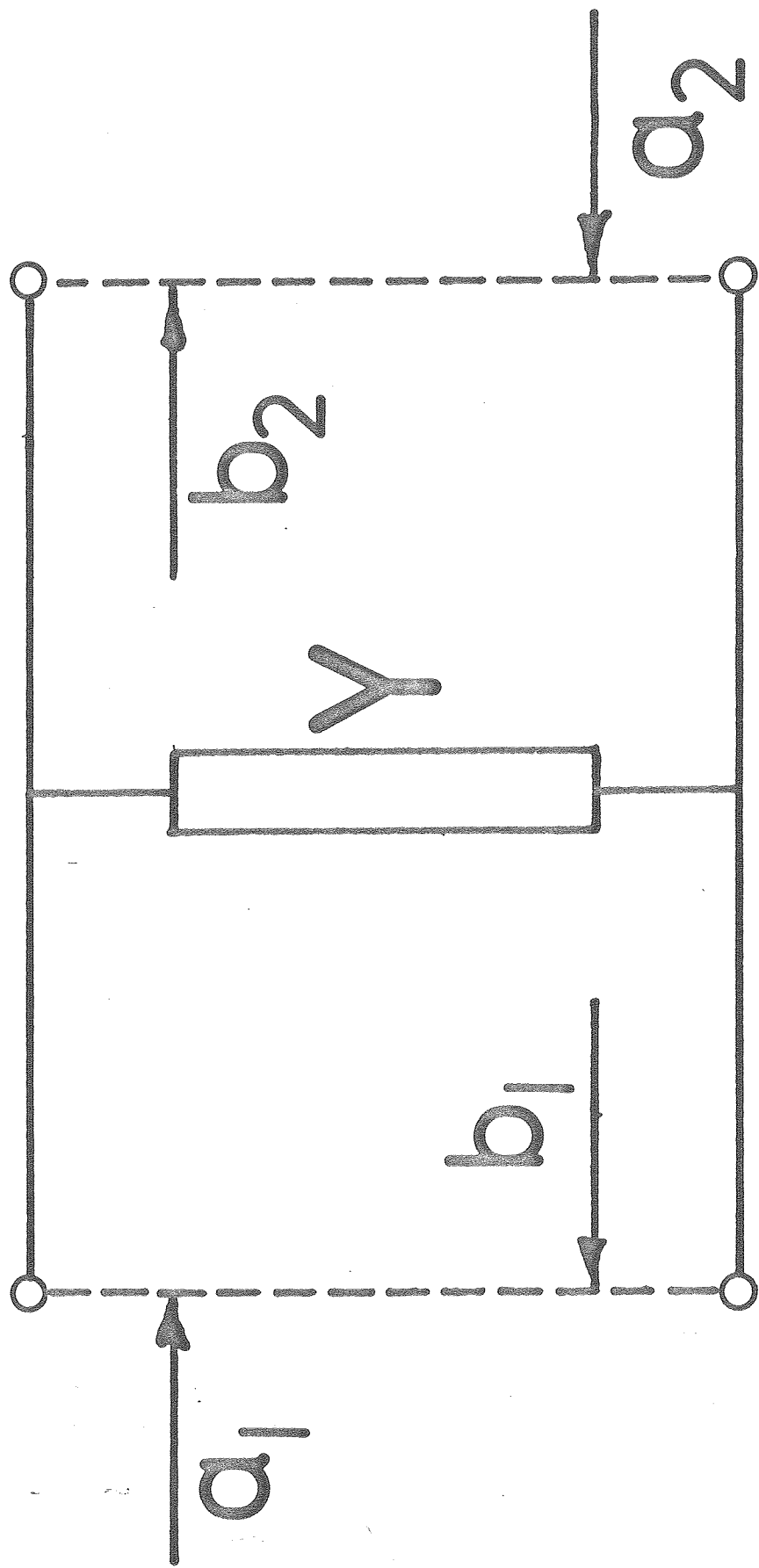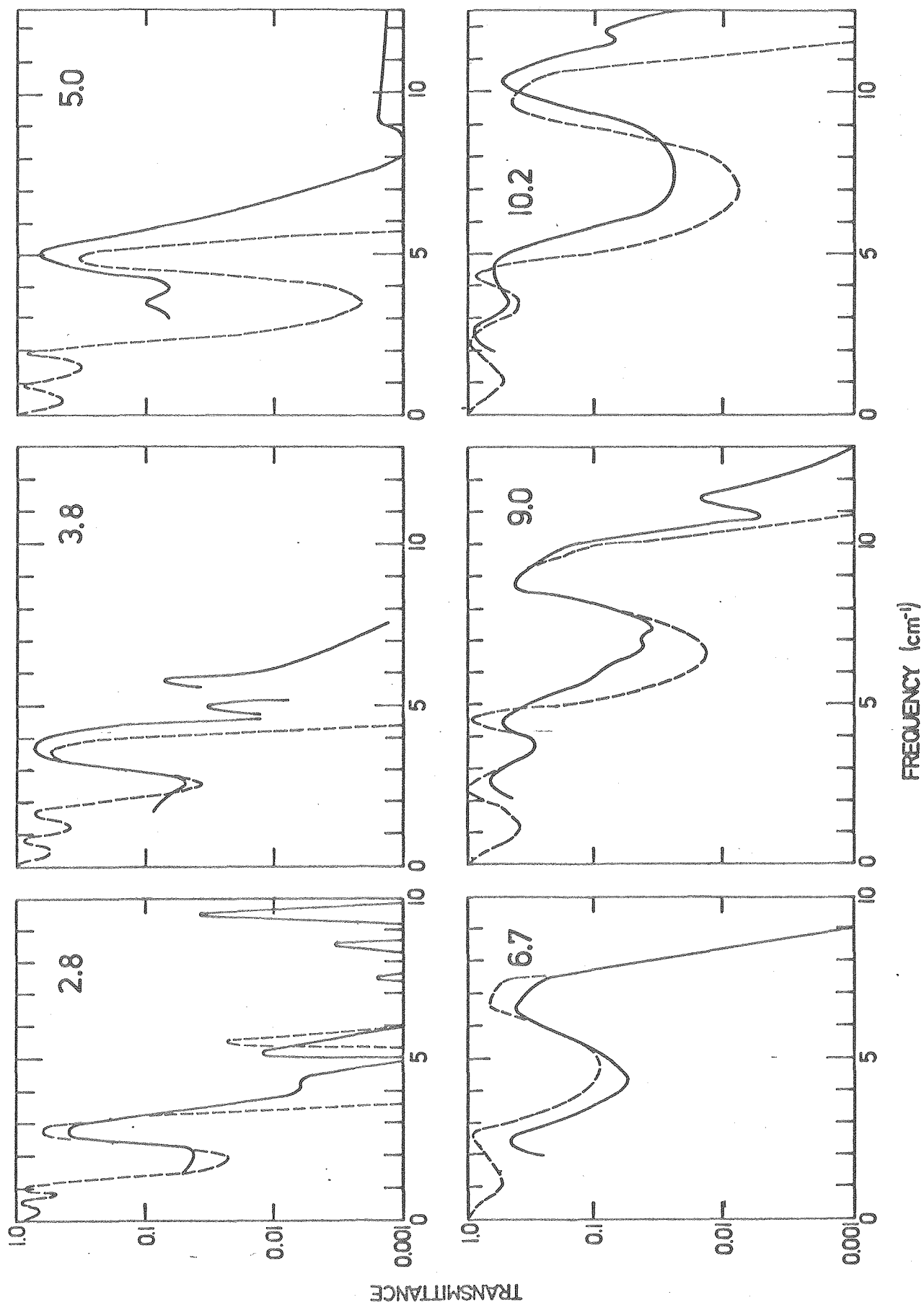
Fig. 1

Fig. 2

Fig. 3

Axis labels: TRANSMITTANCE (vertical), FREQUENCY (cm⁻¹) (horizontal)
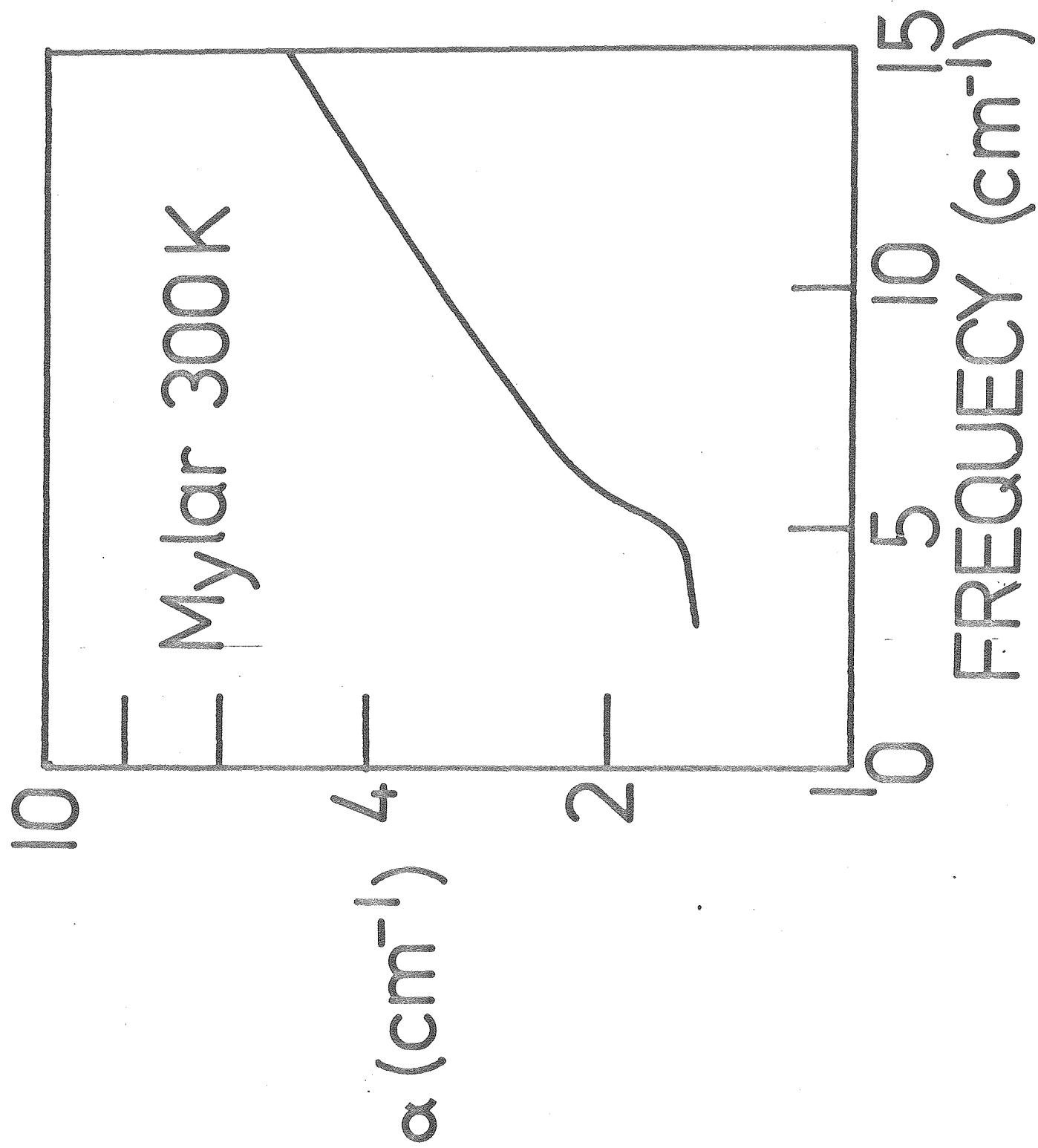
Panel labels: 2.8, 3.8, 5.0, 6.7, 9.0, 10.2

Mylar 300 K

α (cm⁻¹)

FREQUECY (cm⁻¹)

Fig. 4

Fig. 5

Fig. 6

Fig. 7

$R(\nu)$

$\dfrac{\nu}{\left(W\,cm^{-2}sr^{-1}cm^{-1}\right)}$

10^5

10^4

10^3

FREQUENCY (cm⁻¹)

5

10